

# The roughness of stylolites: Implications of 3D high resolution topography measurements

J. Schmittbuhl

*Laboratoire de Géologie, UMR CNRS 8538, Ecole Normale Supérieure,  
24, rue Lhomond, F-75231 Paris Cédex 05,  
France. Email: Jean.Schmittbuhl@ens.fr.*

F. Renard<sup>‡</sup> and J.P. Gratier

*LGIT-CNRS-Observatoire, Université J. Fourier BP 53, F-38041 Grenoble,  
France & <sup>‡</sup>Physics of Geological Processes, University of Oslo, Norway.*

R. Toussaint

*Institute of Physics, University of Oslo,  
PB 1048, Blindern, N-0316 Oslo, Norway.*

(Dated: October 6, 2018)

## Abstract

Stylolites are natural pressure-dissolution surfaces in sedimentary rocks. We present 3D high resolution measurements at laboratory scales of their complex roughness. The topography is shown to be described by a self-affine scaling invariance. At large scales, the Hurst exponent is  $\zeta_1 \approx 0.5$  and very different from that at small scales where  $\zeta_2 \approx 1.2$ . A cross-over length scale at around  $L_c = 1$  mm is well characterized. Measurements are consistent with a Langevin equation that describes the growth of a stylolitic interface as a competition between stabilizing long range elastic interactions at large scales or local surface tension effects at small scales and a destabilizing quenched material disorder.

PACS numbers: 83.80.Ab, 62.20.Mk, 81.40.Np

Stylolites are geological patterns that are very common in polished limestones, a material largely used to construct floors and walls of buildings and monuments. They are observed as thin irregular interfaces that look like printed lines on rock cuts, which is responsible for their name. They are roughly planar structures that are typically perpendicular to the geological load (i.e. lithostatic pressure or tectonic maximum compressive stress). These rock-rock interfaces are formed at shallow depths in the Earth’s crust during deformation of sedimentary rocks and result from a combination of stress-induced dissolution and precipitation processes [1]. They are found in many sedimentary rocks such as limestones, sandstones or evaporites [2] and exist on a very large range of scales, from micro-meters to meters.

Despite their abundance, stylolites are, as mentioned by *Gal et al.* [3], “among the least well-explained of all pressure-solution phenomena”. First they are complex 3D structures that are often only described from 2D cross-sections since they are generally partially sealed [4]. Second, they develop in various geological contexts which lead to very different geometries. Third they are sometimes transformed because of processes like diagenesis and metamorphism that develop after their initiation.

In this Letter we show the first 3D high resolution topography measurements of natural stylolite interfaces that could be fully opened. We characterized the scaling invariance, namely self-affinity, of the morphology and show the presence of a cross-over length scale. We also propose a model of the stylolites roughening. It is based on a Langevin equation that accounts for stress-induced dissolution in a quenched disorder.

The roughness measurements have been performed on three independent stylolite interfaces included in very fine-grained limestone samples from Burgundy area, Vercors, and Jura mountains in France (Fig. 1). The samples have been collected in newly open quarries, thus preserved from late breakage and chemical erosion. The opening procedure was possible for these samples because of the accumulation of undissolved minerals like clays that formed a weak layer along the stylolite interface. The concentration of these minerals provides an estimate of the cumulative strain by dissolution the sample underwent [5]. As shown in Fig. 1, peaks along the interface are randomly distributed in space and of various sizes (up to one centimeter). Large peak magnitudes and local high slopes along the topography makes the roughness measurement difficult and challenging.

We used two different profilometers to sample the stylolite roughness. First, with a mechanical profilometer [6, 7] we extracted four profiles of 1030 points each with a horizontal

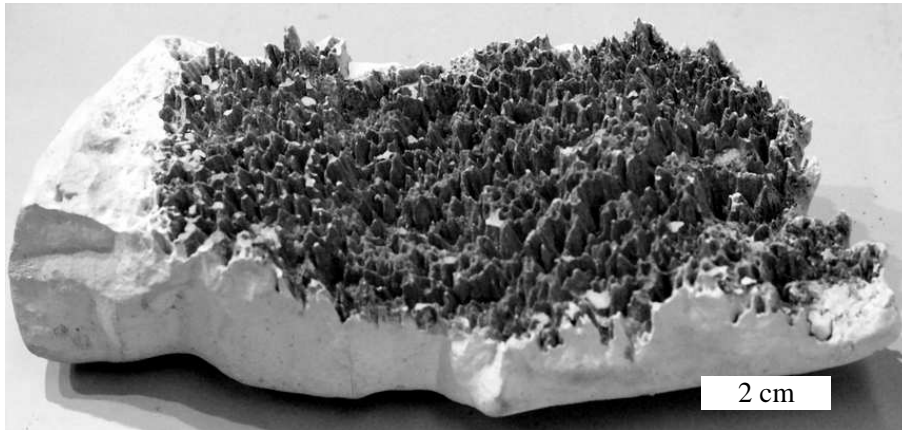


FIG. 1: Picture of a stylolite surface (S12A) in a limestone from Vercors Mountains. Magnitude of the peaks are typically of the order of 6 mm.

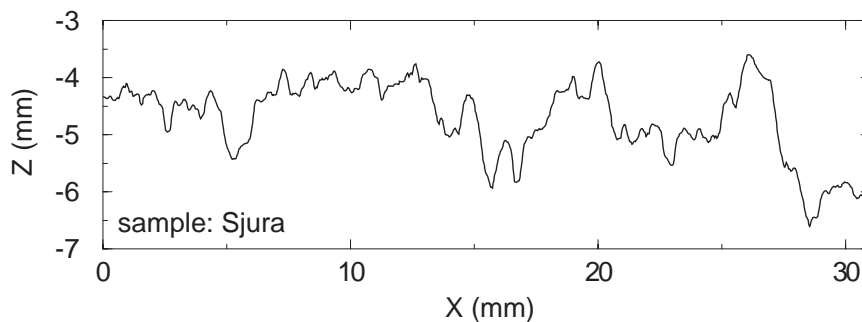


FIG. 2: A 1D profile obtained by a mechanical profilometer (1030 data points -  $\Delta x = 30\mu\text{m}$ ) along a stylolite surface.

step of  $\Delta x = 30 \mu\text{m}$ . The mechanical profilometer measures the surface height from the contact of a needle onto the surface. The radius of the needle tip is  $25 \mu\text{m}$ . The vertical resolution is  $3 \mu\text{m}$  over the available range of  $5 \text{ cm}$ . One of these profiles is shown in Fig. 2. We compare the mechanical measurements to an optical profiling [8]. This technique is based on a laser triangulation of the surface without any contact with the surface. The laser beam is  $30 \mu\text{m}$  wide. Horizontal steps between measurement points were  $\Delta x = \Delta y = 7$  to  $50 \mu\text{m}$  with a vertical resolution of  $2 \mu\text{m}$ . The main advantage of this technique comes from the high acquisition speed that can be performed compared to the mechanical profilometer, since there is no vertical move and on-flight measurements are possible. However, a successful comparison with mechanical measurements is necessary to ensure that optical fluctuations

are height fluctuations and not material property fluctuations. Three independent samples have been measured at very high resolution: one side of a stylolite from Jura mountains (Sjura) with a resolution  $600 \times 600$ , one side of a stylolite from Burgundy area (S15) with a resolution  $8200 \times 4100$  and two opposite surfaces of the same stylolite from Vercors mountains shown in Fig. 1 with a resolution  $2400 \times 1400$  for S12A and  $8200 \times 4100$  for S12B.

We analyzed the height distribution in terms of self-affinity [9] which states that the surface remains statistically unchanged for the transform:  $\Delta x \rightarrow \lambda \Delta x$ ,  $\Delta y \rightarrow \lambda \Delta y$ ,  $\Delta z \rightarrow \lambda^\zeta \Delta z$ , where  $\lambda$  can take any real value. The exponent  $\zeta$  is the so-called Hurst exponent. A 1D Average Wavelet Coefficient technique [10] has been used. For a self-affine profile, the wavelet spectrum behaves as a power law with a slope  $1/2 + \zeta$ , and provides an estimate of the Hurst exponent  $\zeta$ . The spectra clearly exhibit two regimes (Fig. 3). At large length scales, a power law behavior is observed with a slope of 1 in the log-log plot, which is consistent with a Hurst exponent of  $\zeta_1 = 0.5$ . At small length scales, a second power law behavior is observed with a larger slope (1.7) in agreement with a Hurst exponent  $\zeta_2 = 1.2$ . The crossover length scale is sharp and defines a characteristic length scale which is slightly different for the three surfaces,  $L_c \approx 1$  mm.  $L_c$  is several orders of magnitude larger than the grain size and significantly larger than experimental cutoffs. This spectral behavior is observed for both mechanical and optical measurements.

We checked that another analysis technique, namely the Fourier power spectrum, was providing very consistent results. Fig. 4 shows averaged 1D spectra of profiles extracted from the surface Sjura. A self-affine property of the profiles leads to a power-law behavior of the power spectrum as  $P(k) \propto k^{-1-2\zeta}$ [9]. Moreover, average spectra of profiles taken along perpendicular directions provide very consistent results (Fig. 4). Isotropy of scaling invariance is confirmed by the circular symmetry of the 2D power spectrum of the surface.

The second part of the letter is devoted to a modeling of the stylolite roughening. The aim is to understand the origin of the self-affine behaviors and of the characteristic length  $L_c$ . We propose to consider a simple model as a paradigm for an interface growth in an heterogeneous medium like natural rocks. This model aims at providing a framework for future modeling of stylolite formation.

We consider the following geometry: The stylolite interface is assumed to be initiated along the boundary between geological beds. Accordingly it can be approximated as the boundary of a quasi-flat and very elongated fluid pore. The trapped fluid is assumed to

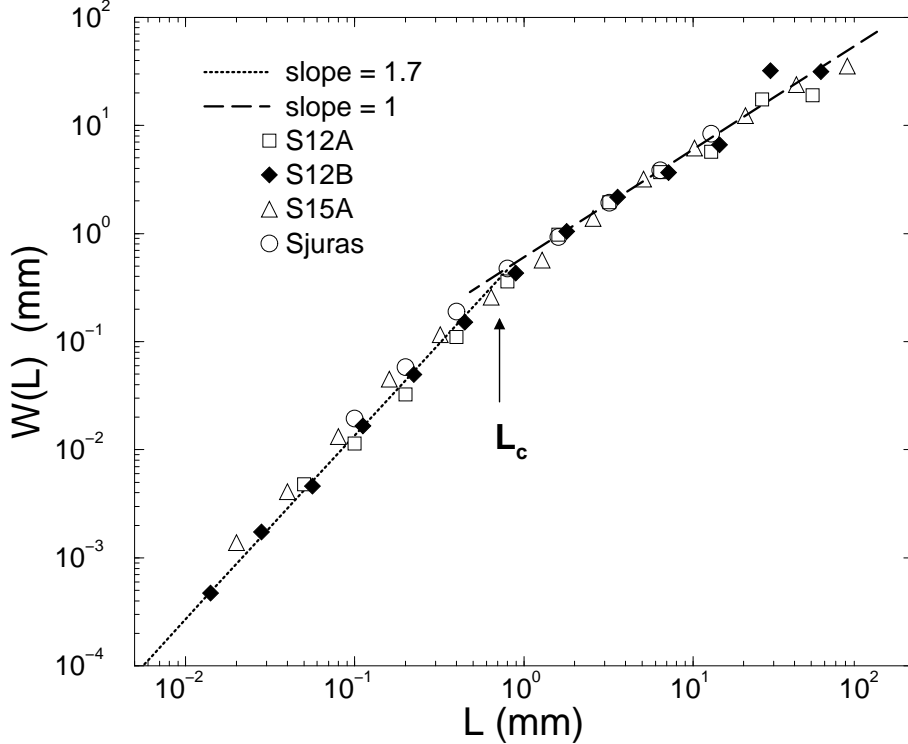


FIG. 3: Averaged wavelet spectra of topographic profiles extracted from four optical maps of stylolite surfaces. Spectra have been normalized to superimpose for large  $L$  on the spectrum of S12A.

form a film and to be at lithostatic pressure. The solid, where this pore is embedded, is supposed to undergo an average stress  $\boldsymbol{\sigma}^0 = \sigma_{zz}^0 \hat{z}\hat{z} + \sigma_{xx}^0 (\hat{x}\hat{x} + \hat{y}\hat{y})$ , where  $\hat{z}$  refers to the direction normal to average stylolite direction and  $\hat{x}$  and  $\hat{y}$  refer to directions along the average stylolite direction. Since stylolites are on average normal to the largest principal stress direction,  $\sigma_s = |\sigma_{zz}^0| - |\sigma_{xx}^0| > 0$ .

Possible solid contacts with the mirror surface on the other side of the fluid film are neglected, considering that such contact points concentrate strain when they occur, and induce faster dissolution of these contacts, thus leading to an essentially lubricated contact zone between neighboring grains: for simplicity, we neglect interactions between the mirror surfaces and assume that the front morphology is to first order dominated by a dissolution process between a fluid film and a single elastic solid.

Assuming a free surface profile  $z(x, t)$ , the normal  $\hat{n}$  to the interface pointing toward the solid is, in the limit of small relief,  $\hat{n} = \hat{z} - (\partial_x z)\hat{x}$ , where we assume plane strain

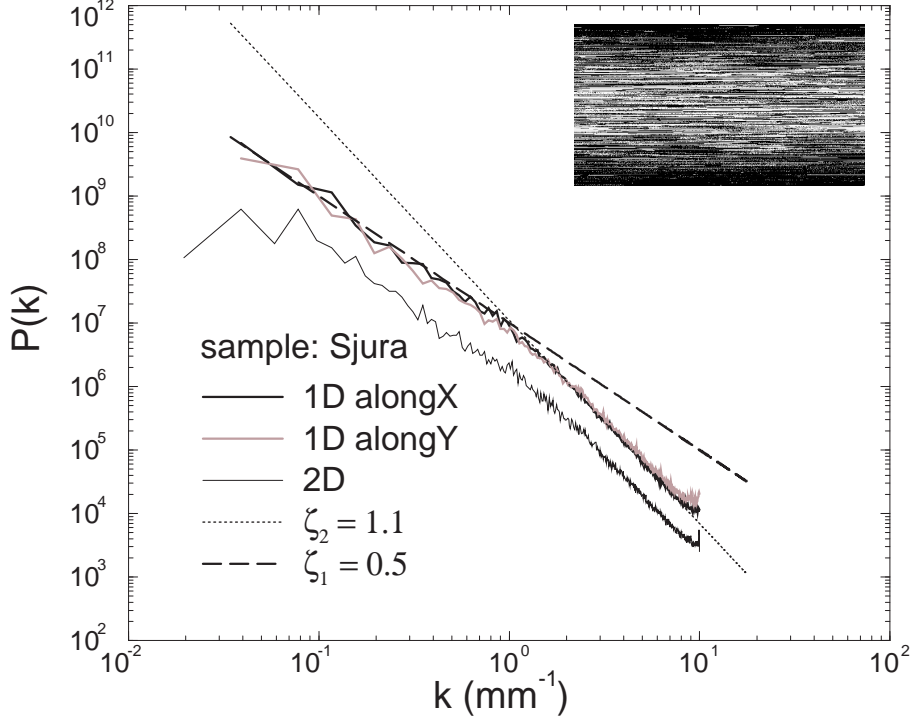


FIG. 4: Fourier power spectra of 1D topographic profiles oriented along two perpendicular directions (X and Y) and of the full 2D surface. The latter was radially integrated to be compared to the 1D power spectra. Inset shows a gray map of the 2D power spectrum. A mirroring technique has been used to reduce non periodic edge effects.

perturbations. The stress state in the solid is expressed as  $\boldsymbol{\sigma} = \boldsymbol{\sigma}^0 + \boldsymbol{\sigma}^1$ , where mechanical equilibrium between solid and fluid requires that  $\boldsymbol{\sigma}^1 \cdot (-\hat{n}) = -\sigma_s(\partial_x z)\hat{x}$ . This stress state results from a surface distribution of tangential force  $-\sigma_s(\partial_x z)\hat{x}$  applied on the quasi-planar boundary of the solid by the fluid, so that using Green's elastostatic function [11] and integrating along the  $y$ -direction, at the surface,  $\sigma_{xz}^1 = \sigma_{zx}^1 = \sigma_s(\partial_x z)$  and  $\sigma_{xx}^1 = \sigma_{yy}^1 = \sigma_s(2\nu/\pi) \int dy(\partial_y z(y))/(x-y)$ , all other components being null.

For small reliefs ( $\|\sigma_1\|/\|\sigma_0\| \ll 1$ ) and to leading order the elastic free energy  $u_e = [(1 + \nu)\sigma_{ij}\sigma_{ij} - \nu\sigma_{kk}\sigma_u]/4E$  can be approximated as  $u_e = u_e^0 + u_e^1$  where from the above,

$$u_e^0 = \alpha p_0^2/E \quad (1)$$

$$u_e^1 = -\beta(p_0\sigma_s/E) \int dy(\partial_y z)/(x-y) \quad (2)$$

with an average solid pressure  $p_0 = -(2\sigma_{xx}^0 + \sigma_{zz}^0)/3$ , and two dimensionless positive constants

$\alpha = [9(1 - 2\nu) + 2(1 + \nu)\sigma_s^2/p_0^2]/12$  and  $\beta = \nu(1 - 2\nu)/\pi$ , where  $E$  is an effective Young's modulus, and  $\nu$  the Poisson coefficient.  $u_e^0$  is the elastic energy from the global tectonic loading and  $u_e^1$  is its local perturbation that results from the interface topography.

The chemical potential difference at the solid/fluid interface that can potentially destabilize the interface can be written as [12]:

$$\Delta\mu = \Omega(u_e + \gamma\kappa) \quad (3)$$

where  $u_e$  is the elastic energy per unit volume in the solid,  $\gamma$  is the surface energy,  $\kappa$  the curvature, and  $\Omega$  a molar volume. We have assumed that gravity effects are negligible. We have also assumed that the matrix of the solid, *i.e.* an assembly of initial sedimentary particles, is sufficiently porous during stylolites initiation to have a bulk diffusion within the material. This assumption is supported by rock thin section observations under an optical microscope [13]. If a bulk diffusion holds in the fluid surrounding the stylolite, the evolution of the interface is directly related to the chemical potential:  $v_n = m\Delta\mu$  where  $v_n$  is the normal dissolution velocity and  $m$  is the mobility [12]. We also neglected the chemical potential evolution within the film since we only aim at describing the initiation of the process under drained conditions.

This homogeneous description thus predicts, for small reliefs,  $\partial_t z = v_0 + m\Omega(u_e^1 + \gamma\partial_{xx}z)$ , with  $v_0 = m\Omega u_e^0$ . Surface tension is a stabilizing term, but it is important to note that the elastic interaction term,  $u_e^1$ , is also stabilizing in the present context. For the present situation, stylolites are perpendicular to the maximum principal stress, and will subsequently be assumed horizontal:  $\sigma_s > 0$ . Considering an elementary departure from a flat interface, such as a fluid intrusion in the solid, *i.e.* a bump with a maximum in  $x$ , such as  $\partial_y z > 0$  for  $y < x$ , and  $\partial_y z < 0$  for  $y > x$ ,  $u_e^1$  is negative in  $x$  and reduces the dissolution speed in the bump at  $x$ . Accordingly, since the problem is linear, elastic interactions are stabilizing for any corrugations of the interface. For vertical stylolites, the picture is opposite ( $\sigma_s < 0$ ) and elastic interactions are destabilizing leading to a lateral expansion of the stylolite.

The homogeneous picture predicts the propagation of a planar dissolution interface driven by the average elastic energy  $u_e^0$ , with an average speed estimated as  $v_0 \approx 8 \cdot 10^{-6}$  m/year where we used  $m = k\Omega/(RT)$ , with a dissolution rate  $k \approx 10^{-4}$  mol/m<sup>2</sup>/s,  $\Omega \approx 4 \cdot 10^{-5}$  m<sup>3</sup>/mol for calcite,  $R$  is the universal gas constant,  $T \approx 300$  K,  $\alpha \approx 0.5$ ,  $E \approx 8 \cdot 10^{10}$  Pa for limestones, a characteristic stress estimated as  $p_0 \approx 25$  MPa, corresponding to a rock at 1

km depth.

To understand the dynamic roughening of stylolites, it is essential to capture the effect of heterogeneities of relevant material properties in the solid, namely  $\nu, E, m$  and  $\gamma$ . We assume the relative variation ( $\delta E/E$  and others) of these properties to be small, and to correspond to independent random variables associated to each constitutive grain of the rock, which are typically  $\ell=10 \mu\text{m}$  sized. At early stages of the process where  $\partial_x z \ll 1$ , we define the dimensionless surface position with respect to the average plane  $z' = (z - v_0 t)/\ell$  and the dimensionless space and time variables  $x' = x/\ell$  and  $t' = t/\tau$  where  $\tau = \ell^2/(\gamma\Omega m)$  to obtain, to leading order in relative fluctuations and typical slopes, for the roughening interface speed:

$$\partial_{t'} z'(x', t') = \partial_{x'} z' - \frac{\ell}{L^*} \int dy' \frac{\partial_{y'} z'}{x' - y'} + \eta(x', z'(x')) \quad (4)$$

where  $L^* = \gamma E/(\beta p_0 \sigma_s)$  and  $\eta = [\alpha \ell p_0/(\beta L^* \sigma_s)] \cdot [(\delta E/E) + (\delta m/m) - (\delta \alpha/\alpha)]$ . In this Langevin equation with quenched noise, the destabilizing random term is balanced by the restoring surface tension term at scales below  $L^*$ , and by the restoring elastic interactions at scales above  $L^*$ . We propose that this critical scale  $L^*$  corresponds to the measured crossover length  $L_c$ . For typical limestones,  $\gamma = 0.27 \text{ J/m}^2$  for a water-calcite surface and  $\nu \approx 0.25$ , so that  $\beta \approx 0.04$  and  $L^* \approx 0.9 \text{ mm}$ , consistently with the above measured. The other characteristic quantities of interest are  $\tau \approx 0.2 \text{ year}$  and the characteristic amplitude of the dimensionless noise  $\eta$  is  $\rho \approx \alpha \ell p_0/(\beta \lambda^* \sigma_s) \approx 0.2$ .

For the Laplacian regime ( $L \ll L^*$ ) and the mechanical regime ( $L \gg L^*$ ), only one of the two restoring terms in Eq. (4) dominates, and these two independent regimes have already been studied. Indeed, the Laplacian regime is nothing else than the Edwards Wilkinson (EW) problem [14] in a quenched noise. In this case the interface is self-affine with an exponent  $\zeta_2 \approx 1.2$  [15]. In the mechanical regime, Eq. (4) is analogous to the quasi-static propagation of an elastic line or a mode I fracture front in a disordered material, and the Hurst exponent is  $\zeta_1 \approx 0.4$  for a kernel similar to Eq. (2) [16, 17, 18, 19].

The roughening amplitude can be obtained by considering the EW equation with quenched noise regime: the characteristic width of the surface measured at scale  $L$  scales as  $w(L)/\ell \approx \rho(L/\ell)^{\zeta_2}$  at saturation, obtained from a flat interface after a saturation time  $\tau_s(L)$  such that  $\tau_s/\tau \approx (L/\ell)^{\zeta_2/\delta}$ , with a dynamic exponent  $\delta \approx 0.8$  [15]. With  $L \approx 1 \text{ mm}$ ,  $\ell \approx 10 \mu\text{m}$  and  $\zeta_2 \approx 1.2$ , this scaling law predicts up to a constant of order unity the

saturation width at cross over scale  $w(L^*) \approx 0.5$  mm and the time to saturation as  $\tau_s \approx 200$  years. This length scale corresponds to the measured one (Fig. 2), and the short saturation time implies that observed stylolites have achieved their saturation width over geological time scales. That the width amplitude is also correctly predicted in the mechanical regime could be checked directly, but is granted by the fact that it is correctly predicted in the Laplacian regime, as well as the crossover scale, which determines entirely the prefactor of the scaling law  $w(L)$  in the  $L > L^*$  regime. In principle, determining  $L^*$  and  $w(L^*)$  could give two independent constraints on both  $p_0$  and  $\sigma_s$ , which could allow to determine both the pressure and differential stress prevailing during the formation of a particular stylolite. However, given the amount of approximations in the involved constants, the only way to test this effect on the cross-over wavelength would be to measure stylolites formed in various geological conditions and study the effect of depth and orientation to the main stress.

In conclusion, we presented a quantitative description of stylolite interfaces. The experimental measurements are 3D high resolution descriptions of the topography of natural stylolites. We show that the surfaces are self-affine but with two regimes. At small scales, the Hurst exponent is unexpectedly high,  $\zeta_2 = 1.2$ , and consistent with a Laplacian regime. At large scales, the stylolites morphology is controlled by long range elastic stress redistributions. In this case the roughening is important with a low Hurst exponent  $\zeta_1 = 0.5$ . The two regimes are separated by a crossover characteristic length  $L_c$ , also predicted by a model based on the description of a stress-induced dissolution, where restoring surface tension effects and elastic interactions compete with a quenched noise. It is important for geological implications to note that  $L_c$  is very sensitive to the average stress  $p_0$ . Indeed, a measurement of  $L_c$  from roughness profiling could provide an estimate of the stress magnitude during the stylolite growth, that is, in the past. Accordingly stylolites could be considered as stress fossils.

We acknowledge D. Rothman, J. Rice, A. Lobkovsky, B. Evans, Y. Bernabé, B. Goffé, H. Perfettini, P. Meakin, and E. Merino for fruitful discussions and two anonymous reviewers for their constructive comments.

---

[1] W. Park and E. Schot, *J. Sed. Pet.* **38**, 175 (1968).

[2] R. Bathurst, *Carbonate sediments and their diagenesis* (Elsevier, Amsterdam, 1971).

- [3] D. Gal, A. Nur, and E. Aharonov, *Geophys. Res. Lett.* **25**, 1237 (1998).
- [4] Z. Karcz and C. H. Scholz, *J. Struc. Geol.* **25**, 1301 (2003).
- [5] F. Renard *et al.*, *J. Geophys. Res.* **108**, B03209 (2004).
- [6] J. Schmittbuhl, F. Schmitt, and C. Scholz, *J. Geophys. Res.* **100**, 5953 (1995).
- [7] J. Lopez and J. Schmittbuhl, *Phys. Rev. E* **57**, 6999 (1998).
- [8] Y. Méheust, Ph.D. thesis, University Paris 11, 2002.
- [9] A. Barabási and H. Stanley, in *Fractal concepts in surface growth*, edited by A. Barabási and H. Stanley (Cambridge University Press, Cambridge, 1995).
- [10] I. Simonsen, A. Hansen, and O. M. Nes, *Phys. Rev. E* **58**, 2779 (1998).
- [11] L. D. Landau and E. M. Lifchitz, *Theory of elasticity*, 3rd ed. (Butterworth-Heinemann, London, 1986).
- [12] K. Kassner *et al.*, *Phys. Rev. E* **63**, 036117 (2001).
- [13] E. Carrio-Schaffhauser and S. Raynaud, *J. Struc. Geol.* **14**, 973 (1992).
- [14] S. Edwards and D. Wilkinson, *Proc. Roy. Soc. A* **381**, 17 (1982).
- [15] S. Roux and A. Hansen, *Journal de Physique I* **4**, 515 (1994).
- [16] J. Schmittbuhl, S. Roux, J. Vilotte, and K. Måløy, *Phys. Rev. Lett.* **74**, 1787 (1995).
- [17] S. Ramanathan and D. Fisher, *Phys. Rev. B* **58**, 6026 (1998).
- [18] A. Tanguy, M. Gounelle, and S. Roux, *Phys. Rev. E* **58**, 1577 (1998).
- [19] A. Rosso and W. Krauth, *Phys. Rev. E* **65**, 025101 (2002).